Published in final edited form as:

Planta Med. 2016 July ; 82(11-12): 1096–1104. doi:10.1055/s-0042-108059.

Isolation of Bioactive Rotenoids and Isoflavonoids from the Fruits of *Millettia caerulea*[*]

Yulin Ren[1], **P. Annécie Benatrehina**[1], **Ulyana Muñoz Acuña**[2], **Chunhua Yuan**[3], **Hee-Byung Chai**[1], **Tran Ngoc Ninh**[4], **Esperanza J. Carcache de Blanco**[1,2], **Djaja D. Soejarto**[5,6], and **A. Douglas Kinghorn**[1]

[1]Division of Medicinal Chemistry and Pharmacognosy, College of Pharmacy, The Ohio State University, Columbus, Ohio 43210, United States

[2]Division of Pharmacy Practice and Administration, College of Pharmacy, The Ohio State University, Columbus, Ohio 43210, United States

[3]Campus Chemical Instrument Center, The Ohio State University, Columbus, Ohio 43210, United States

[4]Institute of Ecology and Biological Resources, Vietnam Academy of Science and Technology, Hoang Quoc Viet, Cau Giay, Hanoi, Vietnam

[5]Department of Medicinal Chemistry and Pharmacognosy, College of Pharmacy, University of Illinois at Chicago, Chicago, Illinois 60612, United States

[6]Science and Education, Field Museum of Natural History, Chicago, IL 60605, United States

Abstract

Three new rotenoids (**1**–**3**), two new isoflavonoids (**4** and **5**), and six known analogues (**6**–**11**) were isolated from a *n*-hexane partition of a methanol extract of the fruits of *Millettia caerulea*, with the structures of the new compounds elucidated by analysis of their spectroscopic data. The relative configurations of the rotenoids were determined by interpretation of their NMR spectroscopic data, and their absolute configurations were established using ECD spectra and specific rotation values. All compounds isolated were evaluated for their cell growth inhibitory activity against the HT-29 human colon cancer cell line, and the known compounds, (−)-3-hydroxyrotenone (**6**) and (−)-rotenone (**7**), were found to be potently active. When tested in a NF-κB inhibition assay, compound **6** showed activity. This compound, along with the new compound, (−)-caeruleanone D (**1**), and the known compound, ichthynone (**8**), exhibited K-Ras inhibitory potency. Further bioactivity studies showed that the new compounds, (−)-3-deoxycaeruleanone D

[*]Dedicated to Professor Dr. Dr. h.c. mult. Kurt Hostettmann in recognition of his outstanding contributions to natural product research

Correspondence: ***Prof. A. Douglas Kinghorn***, Division of Medicinal Chemistry and Pharmacognosy, College of Pharmacy, The Ohio State University, 500 West 12th Avenue, Columbus, Ohio 43210, United States, Phone: + 1 614 247-8094, Fax: + 1 614 247-8642, kinghorn.4@osu.edu.

Supporting information

Mass and NMR spectra of compounds **1–5**; structures, UV and ECD spectra, and diagrams of COSY, the key HMBC and selected NOESY correlations of all isolates; CD or IC_{50} determinations presented as dose-response curves or column graphs; the assignments of the ^{1}H and ^{13}C NMR spectroscopic data and other analytical data of the known compounds isolated from *M. caerulea*.

Conflict of Interest

The authors declare no competing financial interest.

(**2**) and (−)-3-hydroxycaeruleanone A (**3**), and the known compounds **8** and **11** induced quinone reductase in murine Hepa 1c1c7 cells.

Keywords

Fabaceae; *Millettia caerulea*; rotenoids and isoflavonoids; cancer cell growth inhibition; NF-κB and K-Ras inhibition; quinone reductase induction

Introduction

The genus *Millettia*, comprising around 260 species distributed mainly in Africa, Asia, America, and Australia, is a large member of the plant family Fabaceae (subfamily Papilionoideae) [1]. Species of this genus produce rotenoids [2], isoflavonoids [3], and chalcones [4, 5] as characteristic secondary metabolite constituents, which have shown anti-inflammatory [3], anti-insecticidal [1], and antimalarial [5] activities as well as cytotoxicity for cancer cell lines [2, 4, 5]. Millepachine has been identified as a new prenylchalcone from *M. pachycarpa* that exhibited selective cytotoxicity to hepatic cancer cells, as well as *in vivo* antineoplastic activity in a murine xenograft model inoculated by HepG2 hepatocarcinoma cells, when administered intravenously (iv) at a dose of 20 mg/kg per injection [4, 6]. Several different prodrugs of millepachine were investigated, with 3'-hydroxymillepachine-*N*-boc-glycine showing the greatest promise as an anticancer lead compound [7–9].

As part of search for novel anticancer agents from higher plants and other organisms [10], an initial crude chloroform-soluble extract of the fruits of *Millettia caerulea* (Graham) Baker collected in Vietnam was found in a preliminary study to show cytotoxicity toward the HT-29 human colon cancer cell line. Using column chromatography guided by this activity, several rotenoids were purified, of which (−)-3-hydroxyrotenone (**6**) and (−)-rotenone (**7**) were characterized as cytotoxic components of *M. caerulea*, with caeruleanones B and C found to potently induce quinone reductase (QR) *in vitro* [2]. In a continuation of this initial work, as presented herein, a *n*-hexane-soluble extract of *M. caerulea* fruits has been investigated, and several new and known rotenoids and isoflavonoids were identified and evaluated for their cytotoxicity toward HT-29 cells and NF-κB and K-Ras inhibitory and QR induction activities.

Results and Discussion

A *n*-hexane-soluble partition of a methanol extract from the dried fruits of *M. caerulea* was found to show cytotoxicity toward HT-29 cells and was separated by passage over glass columns containing silica gel or Sephadex LH-20. Five new (**1**–**5**) and six known rotenoids and isoflavonoids were isolated, with the latter analogues identified as (−)-3-hydroxyrotenone (**6**) [11, 12], (−)-rotenone (**7**) [12, 13], ichthynone (**8**) [14, 15], (−)-13-homo-13-oxa-2,3-dehydrorotenone (**9**) [16], (−)-2,3-dehydrorotenone (**10**) [17], and (+)-3-hydroxy-α-toxicarol (**11**) (Fig. 1) [18].

Compound **1** was isolated as an amorphous colorless powder. A $C_{23}H_{20}O_8$ molecular formula was deduced from the sodiated molecular ion peak at *m/z* 447.1059 (calcd

447.1050) observed in the HRESIMS, in conjunction with the ^{13}C NMR spectroscopic data. The UV spectrum showed absorption maxima at λ_{max} 248 and 303 nm, consistent with a rotenoid skeleton [2, 15]. This was supported by the absorptions at ν_{max} 3454, 1669, 1640, 1599, and 1503 cm^{-1} in the IR spectrum, corresponding to the presence of hydroxy and conjugated carbonyl groups, a double bond, and an aromatic ring, respectively [19, 20]. Supportive of these inferences, the ^{1}H and ^{13}C NMR spectra of **1** displayed resonances for a rotenoid unit, including an oxygen-bearing methylene group at δ_H 4.48 and 4.61 and δ_C 64.1, an oxygenated methine group at δ_H 4.53 and δ_C 76.4, and three proton singlets at δ_H 6.45, 6.56, and 7.21, along with 12 aromatic carbon resonances in the range δ_C 99.2–152.0 (Tables 1 and 3) [19–21]. In addition, the occurrence of 6-methoxy, 4',5'-methylenedioxy, and 8-(3-methyl-3-*O*-1-buten-1-yl) groups was implied from the $^{13}C/^{1}H$ NMR resonances at δ_C/δ_H 56.5/3.85, 101.5/5.84 and 5.86, and 115.8/6.60, 129.1/5.60, 78.6, 28.6/1.51, and 28.3/1.44, respectively (Tables 1 and 3) [19–21]. This was supported by the HMBC correlations observed between the methoxy protons and C-6, the methylenedioxy protons and C-4' and C-5', H-1" and C-9, and H-2" and C-8, as well the NOESY correlations between the methoxy protons and H-5 (Figs. S7 and S8, Supporting Information).

Comparison of the ^{13}C NMR data of **1** ($C_{23}H_{20}O_8$, Tables 1 and 3) with those of 3-hydroxyerythynone ($C_{24}H_{24}O_8$) showed that both compounds share the same A-, C-, and D-ring substitution patterns, with differences observed for their B-ring [2]. The signals for C-3'–C-6' of **1** appeared at δ_C 99.2, 149.4, 142.4, and 106.0, but those of 3-hydroxyerythynone were reported to resonate at δ_C 101.5, 151.5, 144.4, and 109.9, respectively [2], indicating that **1** is an isomer of 4',5'-demethyl-3-hydroxyerythynone. Further comparison of the ^{13}C NMR data of **1** with those of millettosin ($C_{22}H_{18}O_7$) showed that the major difference was observed for their A-ring substituents. Thus, the signals that appeared at δ_C 107.7, 144.7, 150.9, 109.9, 152.0, and 110.3 for C-5–C-10 of **1** could be contrasted with those reported at δ_C 129.0, 112.3, 161.2, 109.5, 157.0, and 111.4 for the respective carbons of millettosin [2], indicating that **1** is an analogue of 6-methoxymillettosin.

In a NMR spectroscopic study to characterize rotenone epimers, H-6' has been found to resonate at *ca.* δ_H 6.55 of rotenoids with a *cis* coupled C/D ring system (*cis* rotenoids), and is different from an analogues with a *trans* linked C/D ring unit (*trans* rotenoids), where it resonates at *ca.* δ_H 7.77 [22]. This has also been observed for other rotenoids and confirmed by X-ray crystallography of usararotenoid A [23]. Inspection of the structures of *cis* and *trans* rotenoids has shown that the conformation of the C/D ring system of these two compound types is different [24, 25]. In turn, the effect of the C-4 carbonyl group on H-6' [26] is altered, as supported by the different H-6' chemical shift values and conformations of the C/D ring system observed for compounds **9** and **10** [16, 27].

The absolute configuration of rotenone (a *cis* rotenoid containing a C-7 furan-fused 2-methyl-3-*O*-1-buten-4-yl unit, termed here as a “rotenone-like” rotenoid) was established initially as (2*S*,3*S*,2"*R*) by analysis of exhaustive ozonolysis, oxidation, and degradation reactions [28], and confirmed by investigation of the electronic circular dichroism (ECD) spectra of rotenoid and isoflavan compounds [29]. A further extensive ECD study showed that rotenone displays pronounced negative Cotton effects (CEs) at 209 and 276 nm and

positive CE at 237 nm, and relatively weak negative CE 307 nm and positive CEs at 333 and 352 nm, with those its 2,3-di-epimer exhibiting CE bands of opposite signs [30]. A sign inversion of the CEs above 300 nm was observed in "*cis*- 3-hydroxyrotenone-like" rotenoids [20, 30], and a CE sign inversion below 300 nm was found in *cis* "deguelin-like" rotenoids (rotenoids containing a C-7 pyran-fused 3-methyl-3-*O*-1-buten-1-yl unit) [31, 32]. All positive CEs below 300 nm were observed in "*trans*-3-epi-hydroxydeguelin-like" rotenoids [19]. Importantly, the CE curves consistent with those of "*cis*- 3-hydroxyrotenone-like" rotenoids occur in both "rotenone-" and "deguelin-like" rotenoids [19, 20, 31, 32]. Thus, the longer wavelength CE around 350 nm arising from the n→π* transition of the acetophenone chromophore, as indicated by a UV absorption maximum at *ca*. 246 nm [2, 15], and the CE around 320 nm due to the aromatic π→π* transition of the B-ring can be regarded as indicative of the absolute configuration of 3-hydroxyrotenoids [30, 33]. The *cis* nature of **1** was indicated from its H-6' chemical shift at δ_H 6.56 (Table 1) [22–25], and the absolute configuration was defined as (2*S*,3*S*), based on its positive CEs at 203, 218, and 299 nm and negative CE bands at 257 and 366 nm observed in the ECD spectrum (Fig. 2), which were inversed from those reported for a *cis*-(2*R*,3*R*)-"3-hydroxydeguelin-like" rotenoid [32]. Therefore, compound **1** was assigned structurally as (5a*S*,12b*S*)-5a,12b-dihydro-12b-hydroxy-15-methoxy-2,2-dimethyl-2*H*-[1,3]dioxolo[4,5-*g*]pyrano[2,3-*c*:6,5-*f*']bis[1]benzopyran-13(6*H*)-one, and was accorded the trivial name, (−)-caeruleanone D.

Compound **2** was isolated as an amorphous colorless powder, having a molecular formula of $C_{23}H_{20}O_7$, as deduced from the sodiated molecular ion peak at *m/z* 431.1101 (calcd 431.1101) observed in the HRESIMS, and from its ^1H and ^{13}C NMR data (Tables 1 and 3). The similar UV and IR spectra to those of **1** indicated that **2** is also a rotenoid. The molecular formula of **2** ($C_{23}H_{20}O_7$), together with the similar NMR data (Tables 1 and 3) observed for both **1** and **2**, indicated that **2** is a deoxy analogue of **1**. Comparison of the ^1H and ^{13}C NMR data of **2** with those of **1** showed that **2** displayed an additional signal at δ_H 3.88, with the ^{13}C NMR resonances at δ_C 76.4 and 67.8 assigned to C-2 and C-3 of **1** occurring at δ_C 73.3 and 45.2 in **2** (Tables 1 and 3). This indicated that a 3-hydroxy group is absent in **2**, as supported by the ^1H-^1H COSY correlation between H-2 and H-3 and the HMBC correlations observed in the NMR spectra of **2** between H-2 and C-4 and C-1' (Fig. S7, Supporting Information). The *cis* C/D ring system was inferred from the H-6' chemical shift at δ 6.64 (Table 1) [22–25], and a (2*R*,3*R*) absolute configuration was defined from its ECD curve consistent with that of **1** (Fig. 2 and Fig. S9, Supporting Information). Thus, compound **2** [(−)-3-deoxycaeruleanone D] was assigned as (5a*R*, 12b*R*)-5a,12b-dihydro-15-methoxy-2,2-dimethyl-2*H*-[1,3]dioxolo[4,5-*g*]pyrano[2,3-*c*:6,5-*f*']bis[1]benzopyran-13(6*H*)-one.

Compound **3** was isolated as an amorphous colorless powder, with its molecular formula of $C_{28}H_{30}O_8$ deduced from its sodiated molecular ion peak at *m/z* 517.1857 (calcd 517.1833) observed in the HRESIMS and from the ^1H and ^{13}C NMR data (Tables 1 and 3). The UV and IR spectra showed absorption bands indicative of a rotenoid [19, 20], as supported by the similar ^1H and ^{13}C NMR resonances for its B–E-rings to those of **1**. In addition, the ^1H and ^{13}C NMR spectra displayed several pairs of signals at δ_C/δ_H 38.4/2.61 and 2.68 and 39.2/2.37 and 2.72, 117.4/4.76 and 116.3/4.01, 135.7 and 135.6, 25.9/1.58 and 25.4/1.24,

18.0/1.58 and 17.8/1.36 (Tables 1 and 3) assigned to 8,8-di-isoprenyl group and C-7 carbonyl signal at δ_C 195.4 [2], as indicated by the HMBC correlations observed between H-1″a and C-9, H-5 and H-1″b and C-7 (Fig. S7, Supporting Information). Comparison of the ^{13}C NMR spectroscopic data of **3** with those caeruleanone A showed that both compounds exhibited closely comparable resonances except for the C-2 and C-3 signals, which appeared at δ_C 77.0 and 66.6 in **3** rather than at δ_C 73.8 and 43.9, as reported for caeruleanone A [2], indicating that **3** is a C-3 hydroxylated derivative of caeruleanone A, as supported by the ^{1}H-^{1}H COSY and HMBC correlations shown in Fig. S7 (Supporting Information). The *cis* conjugated C/D ring system of **3** could be inferred from H-6' chemical shift at δ 6.48 (Table 1) [22–25], and a (2*S*,3*S*) absolute configuration was determined by its consistent ECD curve with that of **1** (Fig. 2). Thus, compound **3** [(−)-3-hydroxycaeruleanone A] was characterized as [(6a*S*,12a*S*)-rel-6a,12a-dihydro-12a-hydroxy-10-methoxy-8,8-bis(3-methyl-2-buten-1-yl)-[1]benzopyrano[2,3-*c*]-1,3-dioxolo[4,5-*g*][1] benzopyran-9,12(6*H*, 8*H*)-dione].

The unusual *gem*-di-isoprenyl group occurs, for example, among the rotenoids [2], isoflavonoids [34–36], xanthones [37–39], anthronoids [40], and coumarins [41], inclusive of species of the family Calophyllaceae, Clusiaceae, and Fabaceae. The structure of caeruleanone A, the first *gem*-di-isoprenylated rotenoid to have been found, was determined by interpretation of its NMR spectroscopic data and confirmed by X-ray crystallographic analysis [2]. As shown in Fig. 3, compound **3** is proposed as being formed from caeruleanone B, an isolate of *M. caerulea* [2], through a Claisen rearrangement reaction [42]. This proposal can be extended to other *gem-di*-isoprenylated natural products, as evidenced by observation of an accompanying *ortho* carbonyl group or its equilibrated form in these rare naturally occurring compounds [2, 34, 37, 40, 41]. Compound **4** was obtained as an amorphous colorless powder, with its molecular formula of $C_{22}H_{20}O_6$ determined from the sodiated molecular ion peak at *m/z* 403.1154 (calcd 403.1152) observed in the HRESIMS. The UV maxima at λ_{max} 219, 262, 297, and 326 nm, along with the IR absorptions (ν_{max}) at 1636, 1504, and 1469 cm^{-1} showed this compound to be an isoflavonoid, as supported by the characteristic ^{1}H and ^{13}C NMR resonances at $\delta_{H\text{-}2}$ 8.24 and $\delta_{C\text{-}2}$ 153.5 for this type of natural product [34]. The ^{1}H NMR spectrum displayed two singlets at δ_H 7.52 and δ_H 7.12, assignable to H-5 and H-8, respectively, and the resonances for an ABX spin coupled B-ring system at δ_H 7.20 (d, *J* = 1.7 Hz), 6.91 (d, *J* = 8.2 Hz), and 7.11 (dd, *J* = 8.0 and 1.4 Hz) (Table 2), as inferred by the HMBC correlations between H-5 and C-4 and H-8 and C-6 and C-10 and between H-6' and C-3 (Fig. S7, Supporting Information). In addition, 6-methoxy, 3',4'-methylenedioxy, and 7-*O*-isoprenyl groups were indicated from the ^{13}C/^{1}H NMR resonances at δ_C/δ_H 56.3/3.93, 102.1/6.04, 66.8/4.75, 120.0/5.56, 139.2, 25.8/1.81, and 18.3/1.80 (Tables 2 and 3) [5, 34], as supported by the HMBC correlations observed between the methoxy protons and C-6, the methylenedioxy protons and C-3' and C-4', H-1" and C-7, as well the NOESY correlations between the methoxy protons and H-5 (Figs. S7 and S8, Supporting Information). Therefore, compound **4** could be assigned as 3-(1,3-benzodioxol-5-yl)-7-*O*-(3-methyl-2-buten-1-yl)-6-methoxy-4*H*-1-benzopyran-4-one, or 7-*O*-prenyl-3',4'-demethylcladrastin. Compound **5** was isolated as an amorphous colorless powder, having a molecular formula of $C_{23}H_{24}O_6$ deduced from the sodiated molecular ion peak at *m/z* 419.1468 (calcd 419.1465) observed in the HRESIMS and from the ^{1}H and ^{13}C

NMR data (Tables 2 and 3). The UV and IR spectrum showed similar absorption bands to those of **4**, indicating that **5** is a further isoflavonoid. Comparison of the ^{1}H and ^{13}C NMR data with those of **4** showed the signals for their A- and C-rings to be closely similar, with those for the B-ring being different. The $^{13}C/^{1}H$ NMR resonances at δ_C/δ_H 102.1/6.04 assigned to a 3',4'-methylenedioxy group for **4** were found to be replaced by those at δ_C/δ_H 56.1/3.94 and 56.1/3.92 for two methoxy groups in **5**. These methoxy groups could be located at the C-3' and C-4' positions, as supported by the HMBC correlations between these methoxy groups and C-3' and C-4' (Fig. S7, Supporting Information). Thus, compound **5** was defined as 3-(3,4-dimethoxyphenyl)-7-*O*-(3-methyl-2-buten-1-yl)-6-methoxy-4*H*-1-benzopyran-4-one, and was assigned the trivial name, 7-*O*-prenylcladrastin. Previously, several rotenoids, isoflavonoids, and chaconoids were characterized *from Millettia* species through cytotoxicity-guided isolation procedures [e.g. 2, 4]. Consistent with this, in the present study, 11 new and known rotenoids and isoflavonoids were identified from the *n*-hexane-soluble extract of the dried fruits of *M. caerulea* in a similar manner using the HT-29 cell line. The structures of all isolates (Fig. 1) were determined by interpretation of their spectroscopic data or by comparison of these data with reference values [11–18], with the full assignments of the ^{1}H and ^{13}C NMR spectroscopic data listed in Tables 1–3 or S1– S3 (Supporting Information). The relative configuration of the rotenoids **1–3, 6, 7**, and **11** was assigned by their H-6' chemical shift value, which was evidenced as an indicative of *cis* or *trans* C/D-rings of rotenoids [22, 23], with the absolute configuration corroborated by comparison of their ECD and NOESY NMR spectra with those of reference compounds (Fig. 2 and Figs. S8 and S9, Supporting Information). The unusual known compound, oxadehydrorotenone (**9**), which was identified originally from cubé resin, with the structure confirmed by the single crystal X-ray diffraction [16], was isolated herein as the second oxarotenoid from the genus *Millettia* (the first member was isolated from *M. pachycarpa* [4]), but no chalcones were identified from *M. caerulea*, either from our prior work [2] or in the present study.

All chromatographically and spectroscopically pure compounds (purity >95%) isolated from *M. caerulea* were tested for their cell growth inhibitory activity against the HT-29 cell line, using paclitaxel as the positive control [2, 43]. Except for (−)-3-hydroxyrotenone (**6**) and (−)-rotenone (**7**), which were reported earlier to exhibit potent activity toward HT-29 cells but a lack of cytotoxicity against the CCD-112CoN human normal colon cell line [2], all other isolates were found to be inactive (Table 4), indicating that **6** and **7** were responsible for the cytotoxicity observed for the initial *M. caerulea* extract toward HT-29 cells.

Based on previous investigations and the present work, a preliminary structure-activity relationship between rotenoids and their cytotoxicity toward the HT-29 and other human cancer cell lines could be inferred. Compounds **6** and **7** were potently active, but deguelin, tephrosin, (−)-2,3-dehydrorotenone (**10**), and dehydrodeguelin were found to be inactive [2], indicating that both the furan-fused isoprenyl group (F-ring) linked at A-ring and the C-2 and C-3 chiral centers are required for rotenone to mediate its cytotoxicity toward HT-29 cells. Also, an unmodified F-ring has been found to play a critical role in mediating cytotoxicity, as shown earlier for rotenoids of the rotenone, deguelin, oxadehydrorotenoid, and dehydrorotenoid subtypes [12, 24, 25, 44]. The E-ring was found important for (−)-3-

hydroxyrotenone (**6**) to mediate its cytotoxicity against HT-29 cells, as implied by comparison of this activity of **6** (IC_{50} 0.1 μM) with that of 3-hydroxyisomillettone (IC_{50} >20 μM) [2]. Interestingly, several 3-hydroxyrotenone glycosides showed potent cytotoxicity toward the human breast cancer MCF-7 and HCT-116 human colon cancer cell lines, but this same effect was not observed for those analogues with a glucose unit connected to the C-11 and C-3" positions [20]. Consistent with a previous report [12], compound **6** showed slightly more potent activity than **7**, indicating that a C-3 hydroxy group contributes to the cytotoxicity of retonone. Methylation of this group or change of its stereochemistry resulted in a decrease of cytotoxicity against the MCF-7 cell line [25]. Although (−)-13-homo-13-oxa-2,3-dehydrorotenone (**9**), (−)-2,3-dehydrorotenone (**10**), dehydrodeguelin, deguelin, and tephrosin isolated from *M. caerulea* were inactive toward HT-29 cells [2], they have been shown activity towards other mammalian cancer cell lines [4, 12, 16, 24, 25, 44, 45], thereby demonstrating the selective cancer cell cytotoxicity of this compound class.

Several rotenoids have shown toxicity to organisms when they were evaluated in *in vivo* mouse models [24, 45–47]. For example, in a test of acute toxicity to mice, rotenone and deguelin showed LD_{50} values of 2.5 and 5.0 mg/kg by ip administration, respectively [24]. (−)-3-Hydroxyrotenone (**6**) was found to be lethal to mice at a dose of 5 mg/kg (ip) [47], with a dose of less than 4 mg/kg used for deguelin for *in vivo* studies [45, 46]. The cytotoxic dehydrorotenoids and oxarotenoids were found to be non-toxic to mice (LD_{50} >50 mg/kg, ip) [24], indicating the promise of these compounds as potential anticancer leads, if they are subjected to further C- and D- ring-related modifications, following the path of development of millepachine [4, 6–9, 44]. Activation of nuclear factor kappa B (NF-κB), a ubiquitous cellular transcription factor, is associated with induction of antiapoptotic proteins required by cancer cells to maintain viability, thus inhibition of this protein may benefit cancer treatment and has been regarded as a promising target for anticancer drug discovery [48, 49]. To identify their possible mechanism of action, compounds **1, 6, 7, 8**, and **11**, isolated from *M. caerulea* in the present study, were evaluated for their NF-κB inhibitory activity in HeLa cells, using a previously reported procedure, with rocaglamide as positive control [43, 49]. The known cytotoxic rotenoid, **6**, was found to be active, showing an IC_{50} value of 5.3 μM, but all other compounds tested did not show any activity, indicating that **6** may mediate its cytotoxicity partially through a mechanism involved with the inhibition of NF-κB. The 3-hydroxy group seems to be critical in the interaction between compound **6** and the NF-κB protein.

The mutation gene *KRAS* (Kirstein rat sarcoma viral oncogene homologue), found in human cancer cells but not in normal cells, is required for tumor maintenance [50]. As a synthetic lethal partner of *KRAS*, TBK1 (TANK-binding kinase 1) can activate NF-κB to support cell survival, and both TBK1 and NF-κB signaling are essential in *KRAS* mutant tumors [50]. As the protein product *of KRAS*, K-Ras functions as an important target for the discovery of selective cytotoxic lead compounds, with several K-Ras inhibitors found to show antitumor or chemoprevention potential [49–51]. In the present study, compounds **1, 6, 7, 8**, and **11** were evaluated for their K-Ras inhibitory activity in HT-29 cells, using a previously reported procedure, with methyl rocaglate as the positive control [49]. The new compound **1** and the known rotenoid **6** and isoflavonoid **8** were found to be active, showing IC_{50} values of 9.4,

3.1, and 3.7 μM, respectively, but compounds **7** and **11** were inactive (Table 4). This indicates that the cytotoxicity observed for **6** could be associated with K-Ras inhibition, and again the 3-hydroxy group appears to be necessary for the interaction between **6** and K-Ras protein. Following this, it can be inferred that (−)-3-hydroxyrotenone (**6**) mediates its cytotoxicity toward HT-29 cells at least in part through K-Ras inhibition involved in a NF-κB signaling. To the best of our knowledge, this is the first report of the K-Ras inhibitory activity of rotenoids and isoflavonoids. The cancer chemopreventive potential of rotenoids and isoflavonoids has been investigated previously [36, 46]. As representatives, deguelin and millepurone (a new 8,8-di-isoprenylated isoflavonoid) were found to show *in vivo* inhibitory effects in a DMBA/TPA mouse skin carcinogenesis model [36, 46]. As an established biomarker, QR induction has been used to evaluate chemopreventive potential of natural products [52, 53], and several rotenoids isolated previously from *M. caerulea* and *Indigofera spicata* were tested using this induction assay, with some compounds found to show such activity [2, 47]. Following a procedure reported earlier, several additional rotenoids and an isoflavonoid isolated in sufficient quantities in the present study were evaluated by the QR induction assay, using L-sulforaphane as the positive control [2, 47]. Compounds **2, 3, 8**, and **11** were found to be active, showing CD values of 2.2, 2.4, 1.8, and 6.6 μM, respectively, with borderline activity observed for **1** (CD 19.8 μM) (Table 5). All these compounds exhibited low cytotoxicity against Hepa 1c1c7 cells, and the isoflavonoid, ichthynone (**8**), and the new *gem* di-isoprenylated rotenoid, (−)-3-hydroxycaeruleanone A (**3**), were found to be the most potently active in the QR induction assay. These two compounds (**3** and **8**) show some promise as chemopreventive leads.

Materials and Methods

General experimental procedures

Optical rotations were measured on a Perkin-Elmer model 343 polarimeter. UV spectra were recorded on a Hitachi U2910 UV spectrophotometer. ECD measurements were performed on a JASCO J-810 spectropolarimeter. IR spectra were recorded on a Nicolet 6700 FT-IR spectrometer. ^{1}H and ^{13}C, DEPT, HSQC, HMBC, NOESY, and COSY NMR spectra were recorded on a Bruker Avance DRX-400, DRX-700, or a DRX-800 MHz NMR spectrometer. ESIMS, HRESIMS, and MS^2 spectra were measured on a Bruker Maxis 4G Q-TOF mass spectrometer. All mass spectrometric data were obtained in the positive-ion mode using an ESI ion source, with scan ranges (m/z) from 100 to 1000. For MS^2 measurements, a dilute sample (around 1 μM in MeOH) was introduced via a syringe pump at a flow rate of 3 μL/min. Column chromatography was conducted using silica gel (65 × 250 or 230 × 400 mesh, Sorbent Technologies). Analytical thin-layer chromatography (TLC) was performed on precoated silica gel 60 F254 plates (Sorbent Technologies). Sephadex LH-20 was purchased from Amersham Biosciences. For visualization of TLC plates, sulfuric acid reagent was used. Fluorescence was tested using a Spectroline (model ENF-260C) UV light source at 386 nm wavelength. All procedures were carried at room temperature using solvents purchased from commercial sources and employed without further purification.

Plant material

A fruit sample of *Millettia caerulea* (Graham) Baker (Fabaceae-Papilionoideae) was collected on July 28, 2011, at Nui Chua National Park (11° 37.998' N; 109° 09.633' E; Alt.: 70 meters above sea level), Ninh Thuan Province, Vietnam, by Drs. D. D. Soejarto, T. N. Ninh, and B. V. Thanh. A voucher specimen (*DDS 14879*) representing this collection was identified by Dr. D. D. Soejarto and deposited at the John G. Searle Herbarium of the Field Museum of Natural History, Chicago, Illinois, USA, under accession #2300833.

Extraction and isolation

The milled air-dried fruits of *M. caerulea* (sample AA06946, 430 g) were extracted with MeOH (1 L × 6) at room temperature. The solvent was evaporated in vacuo, and the dried MeOH extract (32.9 g, 7.6%) was resuspended in 10% H_2O in MeOH (500 mL) and partitioned with *n*-hexane (300, 300, and 200 mL) to yield a *n*-hexane-soluble residue (D1, 3.3 g, 0.8%), which was washed with a 1% aqueous solution of NaCl, to partially remove tannins. The *n*-hexane-soluble extract (3.0 g) exhibited cytotoxicity toward the HT-29 cell line (IC_{50} 1.5 μg/mL) and was subjected to silica gel column chromatography (2.5 × 45 cm), eluted with a gradient of *n*-hexane–acetone (50:1→1:1; 100 mL each). Eluates were pooled by TLC analysis to give 16 combined fractions, D1F1-D1F16, of which D1F11, D1F12, and D1F13 were deemed cytotoxic toward the HT-29 cell line and selected as target fractions for further investigation.

Fraction D1F11 (0.2 g, IC_{50} 1.5 μg/mL) was chromatographed over a silica gel column (2.5 × 20 cm), eluted with a gradient of CH_2Cl_2–acetone, (100:1→1:1; 50 mL each), to yield five combined subfractions (D1F11F1–D1F11F5). Subfraction D1F11F1 was chromatographed over silica gel, eluted with a gradient of CH_2Cl_2–acetone (100:1→1:1; 20 mL each), and purified by separation over a Sephadex LH-20 column, by eluting with a mixture of CH_2Cl_2-MeOH (1:1, 20 mL each), affording (−)-3-deoxycaeruleanone D (**2**, 1.0 mg). Subfraction D1F11F2 was chromatographed over silica gel, eluted with a gradient of CH_2Cl_2–acetone (100:1→1:1; 20 mL each), and purified by separation over a Sephadex LH-20 column, by eluting with a mixture of CH_2Cl_2-MeOH (1:1, 20 mL each), yielding (−)-3-hydroxycaeruleanone A (**3**, 1.0 mg) and *7-O*-prenyl-3',4'-demethylcladrastin (**4**, 1.0 mg). Using the same procedure, (−)-rotenone (**7**, 35.0 mg) was isolated from subfraction D1F11F3. The combined subfractions D1F11F4 and D1F11F5 were chromatographed over silica gel, eluted with a gradient of CH_2Cl_2–acetone (100:1→1:1; 20 mL each), and purified by separation over a Sephadex LH-20 column, eluted with a mixture of CH_2Cl_2-MeOH (1:1, 50 mL each), producing (−)-7-homo-7-oxa-2,3-dehydrorotenone (**9**, 1.0 mg) and (−)-2,3-dehydrorotenone (**10**, 1.0 mg).

Fraction D1F12 (0.2 g, IC_{50} 0.3 μg/mL) was chromatographed over a silica gel column (2.5 × 20 cm), eluted with a gradient of CH_2Cl_2–acetone (100:1→1:1; 50 mL each), to yield three combined subfractions (D1F12F1–D1F12F3). Subfraction D1F12F1 was chromatographed over silica gel, eluted with a gradient of CH_2Cl_2–acetone (100:1→1:1; 20 mL each), and purified by separation over a Sephadex LH-20 column, by eluting with a mixture of CH_2Cl_2-MeOH (1:1, 50 mL each), affording (+)-3-hydroxy-α-toxicarol (**11**, 4.0 mg). Subfraction D1F12F2 was chromatographed over silica gel, eluted with a gradient of

CH_2Cl_2–acetone (100:1→1:1; 20 mL each), and purified by separation over a Sephadex LH-20 column, by eluting with a mixture of CH_2Cl_2-MeOH (1:1, 50 mL each), yielding (−)-3-hydroxyrotenone (**6**, 17.0 mg). Subfraction D1F12F3 was chromatographed over silica gel, using a gradient of CH_2Cl_2–acetone (100:1→1:1; 20 mL each), and purified by separation over a Sephadex LH-20 column, by eluting with a mixture of CH_2Cl_2-MeOH (1:1, 50 mL each), producing ichthynone (**8**, 5.0 mg). Fraction D1F13 (0.1 g, IC_{50} 0.3 μg/mL) was chromatographed over a silica gel column (2.5 × 20 cm), eluted with a gradient of CH_2Cl_2–acetone (100:1→1:1; 50 mL each), to yield three combined subfractions (D1F12F1–D1F12F3). Subfraction D1F13F1 was chromatographed over silica gel, eluted with a gradient of CH_2Cl_2–acetone (100:1→1:1; 20 mL each), and purified by separation over a Sephadex LH-20 column, by eluting with a mixture of CH_2Cl_2-MeOH (1:1, 50 mL each), affording (−)-caeruleanone D (**1**, 9.0 mg). The combined subfractions D1F13F2 and D1F13F3 were chromatographed over silica gel, eluted with a gradient of CH_2Cl_2–acetone (100:1→1:1; 20 mL each), and purified by separation over a Sephadex LH-20 column, by eluting with a mixture of CH_2Cl_2-MeOH (1:1, 50 mL each), giving 7-*O*-prenylcladrastin (**5**, 1.0 mg) and (−)-3-hydroxyrotenone (**6**, 8.0 mg).

Isolates

(−)-Caeruleanone D (1)—Amorphous colorless powder showing a pink color under UV light at 365 nm; R_f 0.52 (CH_2Cl_2-acetone 15:1); $[\alpha]^{20}_D$ –14.0 (*c* 0.3, $CHCl_3$); UV (MeOH) λ_{max} (log ε) 201 (4.21), 248 (3.97), 303 (3.61) nm; ECD (MeOH, nm) λ_{max} (Δε) 203 (+8.7), 218 (+11.5), 257 (−4.6), 299 (+3.2), 366 (−4.7); IR (dried film) ν_{max} 3454, 1669, 1640, 1599, 1503, 1471 cm^{-1}; ^1H and ^{13}C NMR data, see Tables 1 and 3; positive-ion HRESIMS *m/z* 447.1059, calcd for $C_{23}H_{20}O_8Na$, 447.1050.

(−)-3-Deoxycaeruleanone D (2)—Amorphous colorless powder showing a pink color under UV light at 365 nm; R_f 0.60 (CH_2Cl_2-acetone 15:1); $[\alpha]^{20}_D$ –25.0 (*c* 0.1, $CHCl_3$); UV (MeOH) λ_{max} (log ε) 201 (4.14), 246 (3.89), 301 (3.56) nm; ECD (MeOH, nm) λ_{max} (Δε) 205 (+17.0), 213 (−19.3), 228 (+5.7), 257 (−2.0), 300 (+4.0), 368 (−8.4); IR (dried film) ν_{max} 1672 , 1632, 1596, 1470 cm^{-1}; ^1H and ^{13}C NMR data, see Tables 1 and 3; positive-ion HRESIMS *m/z* 431.1101, calcd for $C_{23}H_{20}O_7Na$, 431.1101.

(−)-3-Hydroxycaeruleanone A (3)—Amorphous colorless powder showing a pink color under UV light at 365 nm; R_f 0.58 (CH_2Cl_2-acetone 15:1); $[\alpha]^{20}_D$ –10.0 (*c* 0.2, $CHCl_3$); UV (MeOH) λ_{max} (log ε) 202 (4.30), 233 (sh, 3.79), 301 (3.79) nm; ECD (MeOH, nm) λ_{max} (Δε) 217 (+5.3), 245 (−1.3), 296 (+2.8), 316 (−2.0), 368 (−1.3); IR (dried film) ν_{max} 3441, 1667, 1627, 1588, 1503, 1482 cm^{-1}; ^1H and ^{13}C NMR data, see Tables 1 and 3; positive-ion HRESIMS *m/z* 517.1857, calcd for $C_{28}H_{30}O_8$ Na, 517.1833.

7-O-Prenyl-3',4'-demethylcladrastin (4)—Amorphous colorless powder showing a dark brown color under UV light at 365 nm; R_f 0.57 (CH_2Cl_2-acetone 15:1); UV (MeOH) λ_{max} (log ε) 206 (4.05), 219 (sh, 3.95), 262 (3.74), 297 (sh, 3.60), 326 (sh, 3.45) nm; IR (dried film) ν_{max} 1636, 1504, 1469 cm^{-1}; ^1H and ^{13}C NMR data, see Tables 2 and 3; positive-ion HRESIMS *m/z* 403.1154, calcd for $C_{22}H_{20}O_6Na$, 403.1152.

7-O-Prenylcladrastin (5)—Amorphous colorless powder showing a dark brown color under UV light at 365 nm; R_f 0.29 (CH_2Cl_2-acetone 15:1); UV (MeOH) λ_{max} (log ε) 201 (4.26), 216 (4.15), 263 (4.04), 288 (sh, 3.82), 321 (3.69) nm; IR (dried film) ν_{max} 1633, 1604, 1515, 1469 cm^{-1}; ^1H and ^{13}C NMR data, see Tables 2 and 3; positive-ion HRESIMS *m/z* 419.1468, calcd for $C_{23}H_{24}O_6Na$, 419.1465.

Assay for cytotoxicity assay against HT-29 cells

Cytotoxicity of the samples was evaluated against HT-29 human colon cancer cells using a reported procedure [43]. The cells were cultured under standard conditions and trypsinized. Then, the harvested cells were added to 96-well plates and treated by the test samples dissolved in DMSO at different concentrations, the positive control, and the negative control (DMSO). The plates were incubated at 37 °C in 5% CO_2 for three days, and then the cells were fixed, incubated at room temperature for 30 min, washed with tap water, dried at room temperature overnight, and dyed using sulforhodamine B. After the dyed cells were lysed in tris-base buffer, the plates were read at 515 nm with an ELISA plate reader. Paclitaxel [Sigma-Aldrich, ≥ 95% (HPLC), powder] was used as a positive control, and the IC_{50} values of the test samples in serial dilutions were calculated using nonlinear regression analysis (Table Curve2Dv4; AISN Software, Inc.).

Enzyme-based ELISA assay for NF-κB inhibition

A NF-κB inhibition assay was carried out using a published procedure, with an EZ-Detect Transcription Factor Assay System ELISA kit (Pierce Biotechnology) [43, 49]. The nuclear extracts of HeLa cells (ATCC, American Type Culture Collection) treated with the positive control and the test samples at four different concentrations were used to determine the specific binding ability of the activated p 65 subunit of NF-κB to the biotinylated-consensus sequence and was measured by detecting the chemiluminescent signal in a Fluostar Optima plate reader (BMG Labtech, Inc.). Rocaglamide was used as a positive control [43, 49].

K-Ras inhibition assay

A K-Ras inhibition assay was carried out using a procedure reported previously [49], using a Ras GTPase Chemi ELISA kit from Active Motif (Carlsbad). After HT-29 cells were treated by the positive control, methyl rocaglate, and the test samples at different concentrations, and stimulated by an epidermal growth factor (EGF) solution (5 ng/mL), the cells were lysed. The protease inhibitor was added in the cell lysate. The protein concentration was determined in each sample, using a Bradford protein assay kit, and the K-Ras activity was tested by using Ras GTPase Chemi ELISA kit from Active Motif (Carlsbad), with addition of primary H-Ras antibody (1:500) and secondary antibody horseradish peroxidase-conjugated (1:5000). The luminescence was detected using a Fluostar Optima plate reader (BMG Labtech, Inc.), after chemiluminescence solution was added.

Assay for quinone reductase induction

The potential quinone reductase induction of the isolates was evaluated following a previously published protocol [47, 52, 53]. After mouse liver cancer Hepa 1c1c7 cells (ATCC CRL-2026) were treated with the test samples for 48 h, the cytotoxicity (IC_{50}) and

quinone reductase induction (CD) of the samples were evaluated, with the chemoprevention index (CI) calculated as a ratio of IC_{50}/CD.

Statistical analysis

The measurements were performed in duplicate or triplicate and are representative of two or three independent experiments, where the values generally agreed within 10%. The dose response curve was calculated for CD or IC_{50} determinations using non-linear regression analysis (Table Curve2DV4; AISN Software Inc.). Differences among samples were assessed by one-way ANOVA followed by Tukey-Kramer's test, and the significance level was set at $p < 0.05$.

Supplementary Material

Refer to Web version on PubMed Central for supplementary material.

Acknowledgments

This investigation was supported by grant P01 CA125066, funded by the National Cancer Institute, NIH, Bethesda, MD. The plant sample of *Millettia caerulea* was collected under a collaborative arrangement between the University of Illinois at Chicago (USA) and the Institute of Ecology and Biological Resources of the Vietnam Academy of Science and Technology, Hanoi (Vietnam). We thank Dr. David Hart, Department of Chemistry and Biochemistry, The Ohio State University, for his suggestions concerning the biogenesis of compound **3**. We are grateful to Dr. C. McElroy, College of Pharmacy, and Drs. A. Somogyi, N. M. Kleinholz, and Y. Cao, of the Mass Spectrometry and Proteomics Facility, the Campus Chemical Instrument Center, The Ohio State University, for access for the 400 MHz NMR and the mass spectrometer instrumentations used in this investigation.

Abbreviations

CE	Cotton effect
DMBA	7,12-dimethylbenz[a]anthracene
ECD	electronic circular dichroism
IC_{50}	concentration that inhibits 50% cell growth, NF-κB, or K-Ras activity.
ip	intraperitoneal
iv	intravenous
KRAS	Kirstein rat sarcoma viral oncogene homologue
K-Ras	protein product of *KRAS* gene
LD_{50}	median or 50% lethal dose
NF-κB	nuclear factor kappa B
QR	quinone reductase
sc	subcutaneous
TPA	12-*O*-tetradecanoylphorbol-13-acetate

References

1. Banzouzi JT, Prost A, Rajemiarimiraho M, Ongoka P. Traditional uses of the African *Millettia* species (Fabaceae). Int J Bot. 2008; 4:406–420.
2. Bueno Pérez L, Pan L, Muñoz Acuña U, Li J, Chai HB, Gallucci JC, Ninh TN, Carcache de Blanco EJ, Soejarto DD, Kinghorn AD. Caeruleanone A, a rotenoid with a new arrangement of the D-ring from the fruits of *Millettia caerulea*. Org Lett. 2014; 16:1462–1465. [PubMed: 24552419]
3. Yankep E, Njamen D, Fotsing MT, Fomum ZT, Mbanya JC, Giner RM, Recio MC, Máñez S, Ríos JL. Griffonianone D, an isoflavone with anti-inflammatory activity from the root bark of *Millettia griffoniana*. J Nat Prod. 2003; 66:1288–1290. [PubMed: 14510620]
4. Ye H, Fu A, Wu W, Li Y, Wang G, Tang M, Li S, He S, Zhong S, Lai H, Yang J, Xiang M, Peng A, Chen L. Cytotoxic and apoptotic effects of constituents from *Millettia pachycarpa* Benth. Fitoterapia. 2012; 83:1402–1408. [PubMed: 22902267]
5. Deyou T, Gumula I, Pang F, Gruhonjic A, Mumo M, Holleran J, Duffy S, Fitzpatrick PA, Heydenreich M, Landberg G, Derese S, Avery V, Rissanen K, Erdélyi M, Yenesew A. Rotenoids, flavonoids, and chalcones from the root bark of *Millettia usaramensis*. J Nat Prod. 2015; 78:2932–2939. [PubMed: 26651537]
6. Wu W, Ye H, Wan L, Han X, Wang G, Hu J, Tang M, Duan X, Fan Y, He S, Huang L, Pei H, Wang X, Li X, Xie C, Zhang R, Yuan Z, Mao Y, Wei Y, Chen L. Millepachine, a novel chalcone, induces G2/M arrest by inhibiting CDK1 activity and causing apoptosis *via* ROS-mitochondrial apoptotic pathway in human hepatocarcinoma cells *in vitro* and *in vivo*. Carcinogenesis. 2013; 34:1636–1643. [PubMed: 23471882]
7. Yang Z, Wu W, Wang J, Liu L, Li L, Yang J, Wang G, Cao D, Zhang R, Tang M, Wen J, Zhu J, Xiang W, Wang F, Ma L, Xiang M, You J, Chen L. Synthesis and biological evaluation of novel millepachine derivatives as a new class of tubulin polymerization inhibitors. J Med Chem. 2014; 57:7977–7989. [PubMed: 25208345]
8. Wang J, Yang Z, Wen J, Ma F, Wang F, Yu K, Tang M, Wu W, Dong Y, Cheng X, Nie C, Chen L. SKLB-M8 induces apoptosis through the AKT/mTOR signaling pathway in melanoma models and inhibits angiogenesis with decrease of ERK1/2 phosphorylation. J Pharmacol Sci. 2014; 126:198–207. [PubMed: 25341684]
9. Wu Y, Cao D, Wang F, Ma L, Gao G, Chen L. Synthesis and evaluation of millepachine amino acid prodrugs with enhanced solubility as antitumor agents. Chem Biol Drug Des. 2015; 86:559–567. [PubMed: 25643726]
10. Kinghorn AD, Carcache de Blanco EJ, Chai HB, Orjala J, Farnsworth NR, Soejarto DD, Oberlies NH, Wani MC, Kroll DJ, Pearce CJ, Swanson SM, Kramer RA, Rose WC, Fairchild CR, Vite GD, Emanuel S, Jarjoura D, Cope FO. Discovery of anticancer agents of diverse natural origin. Pure Appl Chem. 2009; 81:1051–1063. [PubMed: 20046887]
11. Magalhães AF, Tozzi AMGA, Sales BHLN, Magalhães EG. Twenty-three flavonoids from *Lonchocarpus subglaucescens*. Phytochemistry. 1996; 42:1459–1471.
12. Blatt CTT, Chávez D, Chai HB, Graham JG, Cabieses F, Farnsworth NR, Cordell GA, Pezzuto JM, Kinghorn AD. Cytotoxic flavonoids from the stem bark of *Lonchocarpus* aff. *fluvialis*. Phytother Res. 2002; 16:320–325. [PubMed: 12112286]
13. Blaskó G, Shieh HL, Pezzuto JM, Cordell GA. ^{13}C-NMR spectral assignment and evaluation of the cytotoxic potential of rotenone. J Nat Prod. 1989; 52:1363–1366. [PubMed: 2614425]
14. Schwarz JSP, Cohen AI, Ollis WD, Kaczka EA, Jackman LM. The extractives of *Piscidia erythrina* L.-I the constitution of ichthynone. Tetrahedron. 1964; 20:1317–1330.
15. Tahara S, Narita E, Ingham JL, Mizutani J. New rotenoids from the root bark of Jamaican dogwood (*Piscidia erythrina* L). Z Naturforsch C: J Biosci. 1990; 45:154–160.
16. Fang N, Casida JE. Novel bioactive cubé; insecticide constituents: isolation and preparation of 13-homo-13-oxa-6a,12a-dehydrorotenoids. J Org Chem. 1997; 62:350–353. [PubMed: 11671409]
17. Arriaga AMC, Lima JQ, Vasconcelos JN, de Oliveira MCF, Andrade-Neto M, Santiago GMP, Uchoa DEA, Malcher GT, Mafezoli J, Braz-Filho R. Unequivocal assignments of flavonoids from *Tephrosia* sp. (Fabaceae). Magn Reson Chem. 2009; 47:537–540. [PubMed: 19306481]

18. Andrei CC, Vieira PC, Fernandes JB, da Silva MFDGF, Fo ER. Dimethylchromene rotenoids from *Tephrosia candida*. Phytochemistry. 1997; 46:1081–1085.
19. Yenesew A, Midiwo JO, Waterman PG. Rotenoids, isoflavones and chalcones from the stem bark of *Millettia usaramensis* subspecies *usaramensis*. Phytochemistry. 1998; 47:295–300.
20. Wu X, Liao HB, Li GQ, Liu Y, Cui L, Wu KF, Zhu XH, Zeng XB. Cytotoxic rotenoid glycosides from the seeds of *Amorpha fruticosa*. Fitoterapia. 2015; 100:75–80. [PubMed: 25449424]
21. Gottlieb HE, Kotlyar V, Nudelman A. NMR chemical shifts of common laboratory solvents as trace impurities. J Org Chem. 1997; 62:7512–7515. [PubMed: 11671879]
22. Abidi SL, Abidi MS. ^{13}C NMR spectral characterization of epimeric rotenone and some related tetrahydrobenzopyranofurobenzopyranones. J Heterocyclic Chem. 1983; 20:1687–1692.
23. Yenesew A, Derese S, Midiwo JO, Oketch-Rabah HA, Lisgarten J, Palmer R, Heydenreich M, Peter MG, Akala H, Wangui J, Liyala P, Waters NC. Anti-plasmodial activities and X-ray crystal structures of rotenoids from *Millettia usaramensis* subspecies *usaramensis*. Phytochemistry. 2003; 64:773–779. [PubMed: 13679101]
24. Fang N, Rowlands JC, Casida JE. Anomalous structure-activity relationships of 13-homo-13-oxarotenoids and 13-homo-13-oxadehydrorotenoids. Chem Res Toxicol. 1997; 10:853–858. [PubMed: 9282833]
25. Fang N, Casida JE. Cubé resin: insecticide: identification and biological activity of 29 rotenoid constituents. J Agric Food Chem. 1999; 47:2130–2136. [PubMed: 10552508]
26. Combrisson S, Roques BP. Overhauser effect (OE), PMR relaxation times and ^{13}C NMR chemical shifts in amide conformation. I. Theoretical study of OE in exchanging systems. Conformational study of aromatic amides (acetylpyrroles) and α,β-unsaturated amides (N-acylindolines and N-acyltetrahydroquinolines). Tetrahedron. 1976; 32:1507–1516.
27. Teerawatananond T, Chaichit N, Muangsin N. Co-crystal structure of 11-hydroxy-2,3,9-trimethoxy-6*H*-chromeno[3,4-*b*]chromen-12-one and 11-hydroxy-2,3,9-trimethoxy-chromeno[3,4-*b*]chromene-6,12-dione. J Chem Crystalllogr. 2010; 40:591–596.
28. Büchi G, Crombie L, Godin PJ, Kaltenbronn JS, Siddalingaiah KS, Whiting DA. The absolute configuration of rotenone. J Chem Soc. 1961; 1961:2843–2860.
29. Verbit L, Clark-Lewis JW. Optically active aromatic chromophores. VIII. studies in the isoflavanoid and rotenoid series. Tetrahedron. 1968; 24:5519–5527.
30. Kostova I, Berova N, Ivanov P, Mikhova B, Rakovska R. Stereochemical studies of some 12a-substituted rotenoid derivatives. Croatica Chem Acta. 1991; 64:637–647.
31. Wangensteen H, Alamgir M, Rajia S, Samuelsen AB, Malterud KE. Rotenoids and isoflavones from *Sarcolobus globosus*. Planta Med. 2005; 71:754–758. [PubMed: 16142641]
32. Nunes e Vasconcelos J, Santiago GMP, Lima JQ, Mafezoli J, Gomes de Lemos TL, Lopes da Silva FR, Lima MAS, Pimenta ATÁ, Braz-Filho R, Arriaga AMC, Cesarin-Sobrinho D. Rotenoids from *Tephrosia toxicaria* with larvicidal activity against *Aedes aegypti*, the main vector of dengue fever. Quim Nova. 2012; 35:1097–1100.
33. Slade D, Ferreira D, Marais JPJ. Circular dichroism, a powerful tool for the assessment of absolute configuration of flavonoids. Phytochemistry. 2005; 66:2177–2215. [PubMed: 16153414]
34. Yankep E, Mbafor JT, Fomum ZT, Steinbeck C, Messanga BB, Nyasse B, Budzikiewicz H, Lenz C, Schmickler H. Further isoflavonoid metabolites from *Millettia griffoniana* (Baill.). Phytochemistry. 2001; 56:363–368. [PubMed: 11249102]
35. Wanda GJMK, Starcke S, Zierau O, Njamen D, Richter T, Vollmer G. Estrogenic activity of griffonianone C, an isoflavone from the root bark of *Millettia griffoniana:* regulation of the expression of estrogen responsive genes in uterus and liver of ovariectomized rats. Planta Med. 2007; 73:512–518. [PubMed: 17486534]
36. Ito C, Itoigawa M, Tan HTW, Tokuda H, Yang Mou X, Mukainaka T, Ishikawa T, Nishino H, Furukawa H. Anti-tumor-promoting effects of isoflavonoids on Epstein-Barr virus activation and two-stage mouse skin carcinogenesis. Cancer Lett. 2000; 152:187–192. [PubMed: 10773411]
37. Azebaze AGB, Meyer M, Valentin A, Nguemfo EL, Fomum ZT, Nkengfack AE. Prenylated xanthone derivatives with antiplasmodial activity from *Allanblackia monticola* STANER L.C. Chem Pharm Bull. 2006; 54:111–113. [PubMed: 16394561]

38. Menasria F, Azebaze AGB, Billard C, Faussat AM, Nkengfack AE, Meyer M, Kolb JP. Apoptotic effects on B-cell chronic lymphocytic leukemia (B-CLL) cells of heterocyclic compounds isolated from Guttiferae. Leukemia Res. 2008; 32:1914–1926. [PubMed: 18656257]
39. Loisel S, Le Ster K, Meyer M, Berthou C, Youinou P, Kolb JP, Billard C. Therapeutic activity of two xanthones in a xenograft murine model of human chronic lymphocytic leukemia. J Hematol Oncol. 2010; 3:49. [PubMed: 21138552]
40. Hussein AA, Bozzi B, Correa M, Capson TL, Kursar TA, Coley PD, Solis PN, Gupta MP. Bioactive constituents from three *Vismia* species. J Nat Prod. 2003; 66:858–860. [PubMed: 12828475]
41. Rouger C, Derbré S, Charreau B, Pabois A, Cauchy T, Litaudon M, Awang K, Richomme P. Lepidotol A *from Mesua lepidota* inhibits inflammatory and immune mediators in human endothelial cells. J Nat Prod. 2015; 78:2187–2197. [PubMed: 26301802]
42. Rehbein J, Hiersemann M. Claisen rearrangement of aliphatic allyl vinyl ethers from 1912 to 2012: 100 years of electrophilic catalysis. Synthesis. 2013; 45:1121–1159.
43. Ren Y, Muñoz Acuña U, Jiménez F, García R, Mejía M, Chai HB, Gallucci JC, Farnsworth NR, Soejarto DD, Carcache de Blanco EJ, Kinghorn AD. Cytotoxic and NF-κB inhibitory sesquiterpene lactones from *Piptocoma rufescens*. Tetrahedron. 2012; 68:2671–2678. [PubMed: 22685350]
44. Cheenpracha S, Karalai C, Ponglimanont C, Chantrapromma K. Cytotoxic rotenoloids from the stems of *Derris trifoliata*. Can J Chem. 2007; 85:1019–1022.
45. Hsu YC, Chiang JH, Yu CS, Hsia TC, Wu RSC, Lien JC, Lai KC, Yu FS, Chung JG. Antitumor effects of deguelin on H460 human lung cancer cells *in vitro* and *in vivo:* roles of apoptotic cell death and H460 tumor xenografts model. Environ Toxicol. 2015; 30
46. Udeani GO, Gerhäuser C, Thomas CF, Moon RC, Kosmeder JW, Kinghorn AD, Moriarty RM, Pezzuto JM. Cancer chemopreventive activity mediated by deguelin, a naturally occurring rotenoid. Cancer Res. 1997; 57:3424–3428. [PubMed: 9270008]
47. Bueno Pérez L, Li J, Lantvit DD, Pan L, Ninh TN, Chai HB, Soejarto DD, Swanson SM, Lucas DM, Kinghorn AD. Bioactive constituents of *Indigofera spicata*. J Nat Prod. 2013; 76:1498–1504. [PubMed: 23895019]
48. Garg A, Aggarwal BB. Nuclear transcription factor-κB as a target for cancer drug development. Leukemia. 2002; 16:1053–1068. [PubMed: 12040437]
49. Muñoz Acuña U, Matthew S, Pan L, Kinghorn AD, Swanson SM, Carcache de Blanco EJ. Apoptosis induction by 13-acetoxyrolandrolide through the mitochondrial intrinsic pathway. Phytother Res. 2014; 28:1045–1053. [PubMed: 24338805]
50. Baines AT, Xu D, Der CJ. Inhibition of Ras for cancer treatment: the search continues. Future Med Chem. 2011; 3:1787–1808. [PubMed: 22004085]
51. Appari M, Babu KR, Kaczorowski A, Gross W, Herr I. Sulforaphane, quercetin, and catechins complement each other in elimination of advanced pancreatic cancer by miR-let-7 induction and K-ras inhibition. Int J Oncol. 2014; 45:1391–1400. [PubMed: 25017900]
52. De Long MJ, Prochaska HJ, Talalay P. Induction of NAD(P)H:quinone reductase in murine hepatoma cells by phenolic antioxidants, azo dyes, and other chemoprotectors: a model system for the study of anticarcinogens. Proc Natl Acad Sci USA. 1986; 83:787–791. [PubMed: 3080750]
53. Cuendet M, Oteham CP, Moon RC, Pezzuto JM. Quinone reductase induction as a biomarker for cancer chemoprevention. J Nat Prod. 2006; 69:460–463. [PubMed: 16562858]

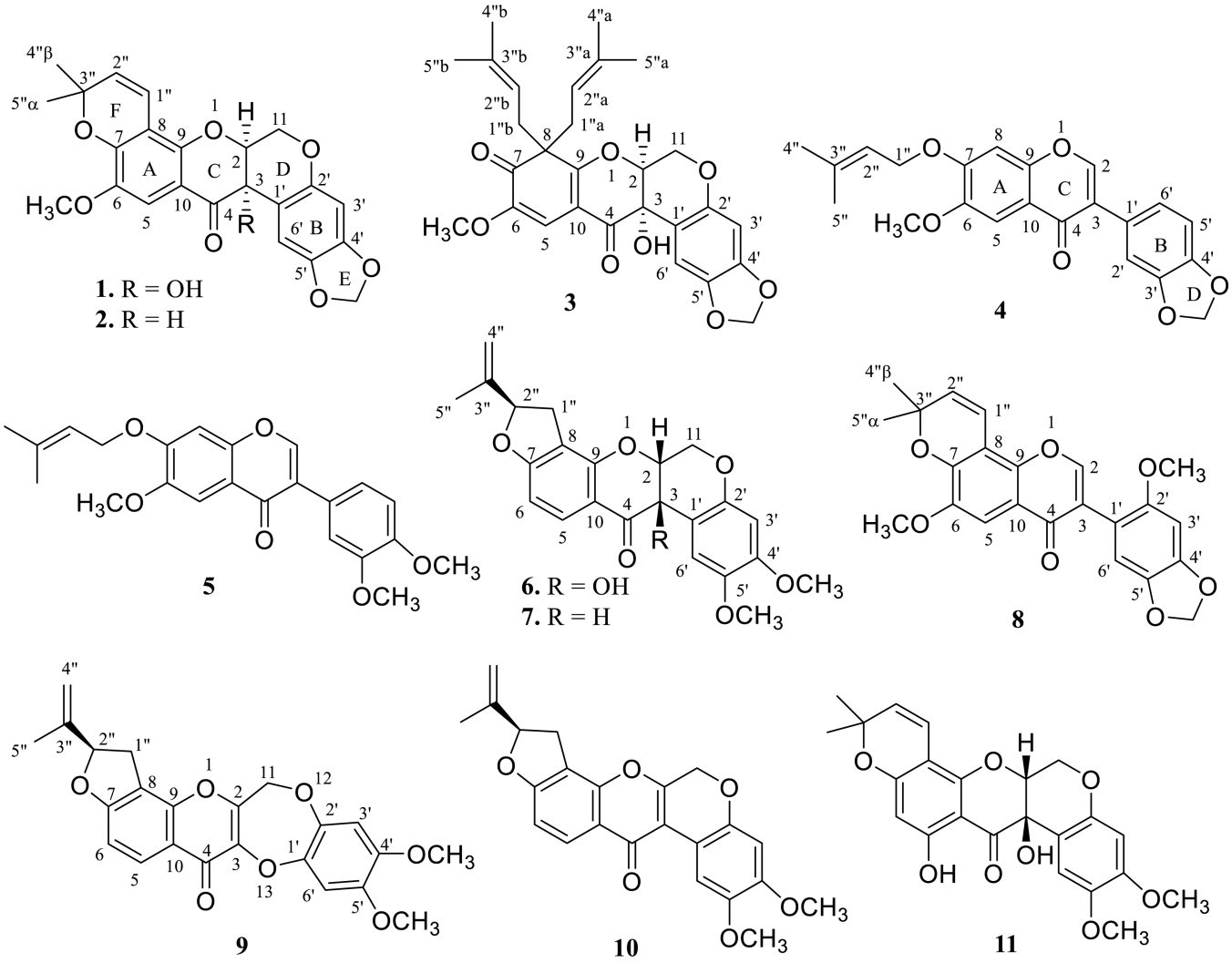

Fig. 1.

Chemical structures of compounds **1**–**11** isolated from *Millettia caerulea*.

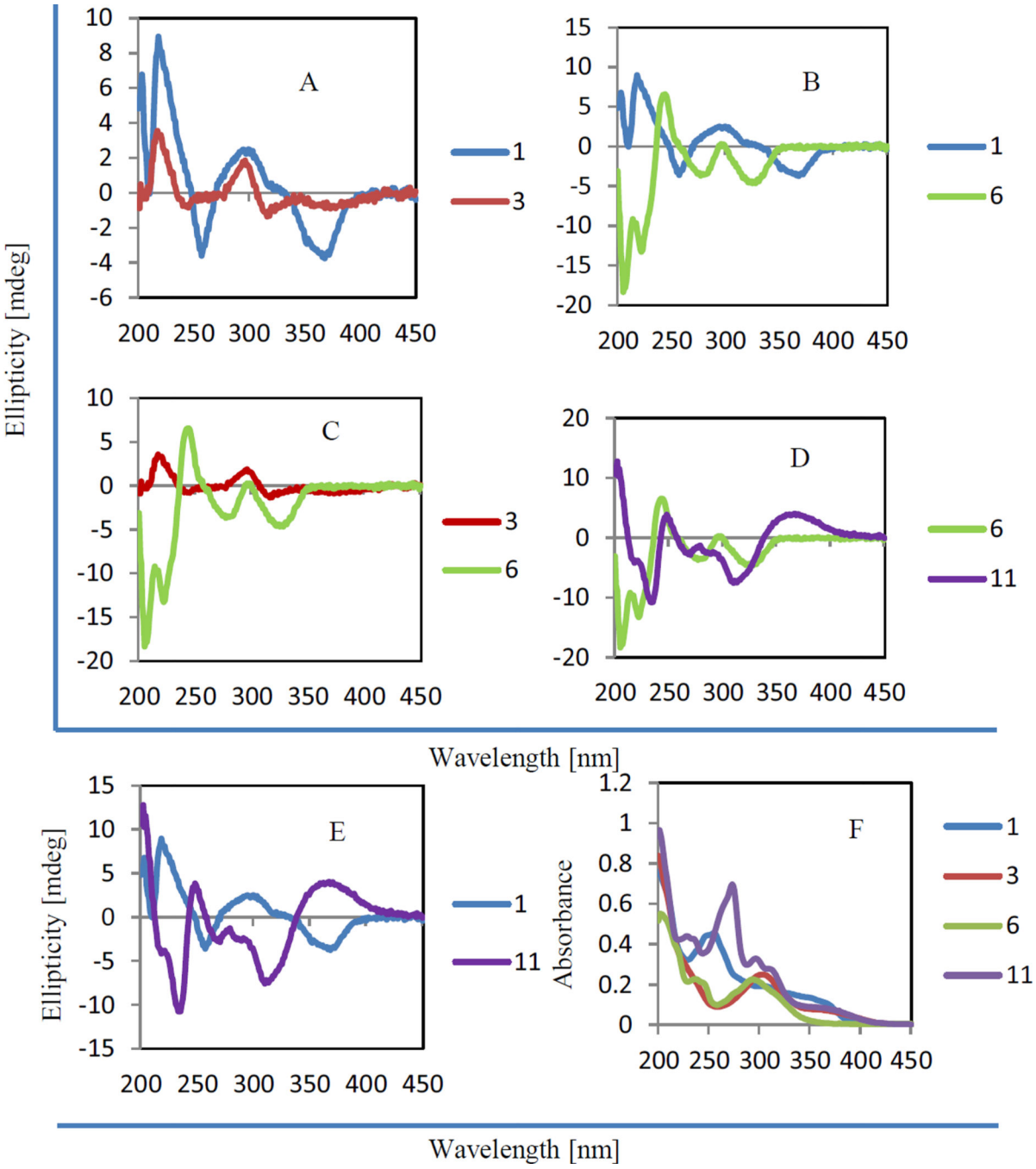

Fig. 2.

ECD (A–E) and UV (F) spectra of compounds **1, 3, 6**, and **11**. The ECD spectra were measured between 450 and 200 nm at room temperature using MeOH solution in a cell of 0.5 cm pathlength, with scanning speed of 50 nm/min and three accumulations, and corrected by subtracting a spectrum of the appropriate solution in the absence of the samples recorded under identical conditions. The UV spectra were recorded in MeOH in a range 200–450 nm with MeOH used as the reference.

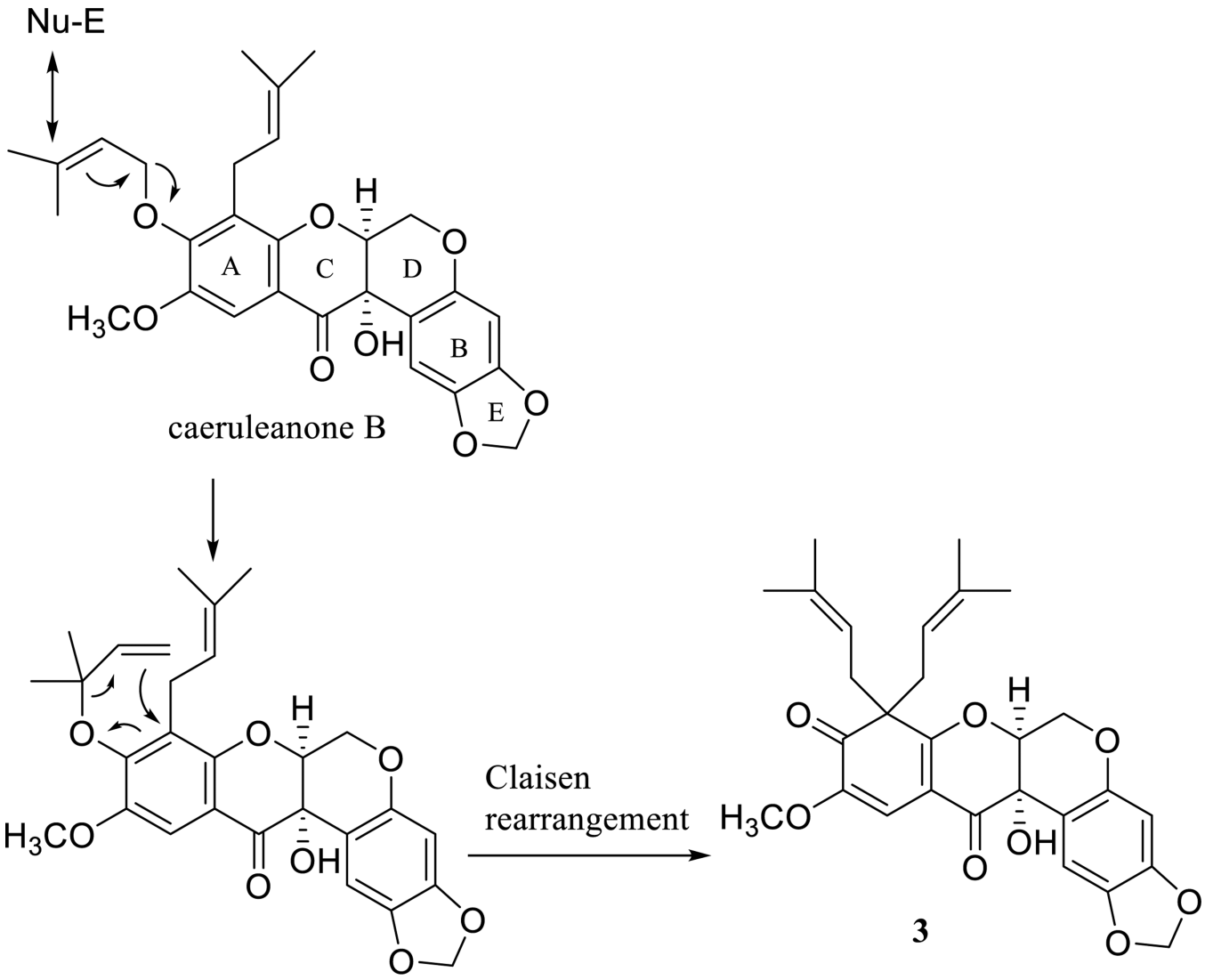

Fig. 3.
Plausible biogenesis of **3**. Compound **3** was proposed to be formed from caeruleanone B through a Claisen rearrangement reaction.

Table 1

^{1}H NMR spectroscopic data of 1–3 (δ_H, *J*, Hz)[a].

Pos.	1[b]	2[c]	3[b]
2	4.53 m	5.09 m	4.49 m
3		3.88 d (3.9)	
5	7.21 s	7.23 s	6.59 s
11	4.48 d (12.2)	4.30 d (12.3)	4.47 d (12.2)
	4.61 dd (12.2,	4.64 dd (12.2,	4.61 dd (12.4, 2.6)
	2.4)	2.8)	
3'	6.45 s	6.39 s	6.45 s
6'	6.56 s	6.65 s	6.48 s
1"/1a"	6.60 d (10.1)	6.64 d (10.2)	2.61 m 2.68 m
2"/2a"	5.60 d (10.1)	5.75 d (10.1)	4.76 t (7.2)
4"/4a"	1.51 s	1.47 (β) s	1.58 s
5"/5a"	1.44 s	1.38 (α) s	1.58 s
1b"			2.37 m 2.72 m
2b"			4.01 t (7.6)
4b"			1.24 s
5b"			1.36 s
OH-3			4.33 s
OCH_3-6	3.85 s	3.80 s	3.72 s
OCH_2O- 4',5'	5.84 d (1.2) 5.86 d (1.2)	5.84 s 5.90 s	5.84 br s 5.89 br s

[a] Overlapped signals were assigned from ^{1}H-^{1}H COSY, HSQC, and HMBC spectra without designating multiplicity

[b] Data (δ) measured in $CDCl_3$ at 400.13 MHz (Bruker DRX) and referenced to the solvent residual peak at δ 7.26 [21]

[c] Data (δ) measured in acetone-d_6 at 800.13 MHz (Bruker DRX) and referenced to the solvent residual peak at δ 2.05 [21]

Table 2

^{1}H NMR spectroscopic data of **4** and **5** [δ_H, (*J*, Hz)][a].

Pos.	4[b]	5[c]
2	8.24 s	7.97 s
5	7.52 s	7.62 s
8	7.12 s	6.88 s
2'	7.20 d (1.7)	7.26 overlapped
5'	6.91 d (8.2)	6.94 d (8.3)
6'	7.11 dd (8.0, 1.4)	7.06 dd (8.2, 1.8)
1"	4.75 d (5.3)	4.70 d (6.4)
2"	5.56 m	5.56 t (6.3)
4"	1.81 s	1.82 s
5"	1.80 s	1.80 s
OCH_3-6	3.93 s	3.98 s
OCH_3-3'		3.94 s
OCH_3-4'		3.92 s
OCH_2O-3',4'	6.04	

[a]Overlapped signals were assigned from ^{1}H-^{1}H COSY, HSQC, and HMBC spectra without designating multiplicity

[b]Data (δ) measured in acetone-d_6 at 400.13 MHz (Bruker DRX) and referenced to the solvent residual peak at δ 2.05 [21]

[c]Data (δ) measured in in $CDCl_3$ at 400.13 MHz (Bruker DRX) and referenced to the solvent residual peak at δ 7.26 [21]

Table 3

^{13}C NMR spectroscopic data of **1–5** (δ_C, type)[a].

Pos.	1[b]	2[c]	3[b]	4[c]	5[b]
2	76.4 CH	73.3 CH	77.0 CH	153.5 CH	152.1 CH
3	67.8 C	45.2 CH	66.6 C	124.6 C	125.1 C
4	191.3 C	189.6 C	189.2 C	175.2 C	175.8 C
5	107.7 CH	109.1 CH	107.3 CH	105.4 CH	104.9 CH
6	144.7 C	145.2 C	148.6 C	149.2 C	148.2 C
7	150.9 C	150.7 C	195.4 C	154.9 C	153.8 C
8	109.9 C	110.9 C	60.2 C	101.7 CH	100.6 CH
9	152.0 C	152.8 C	174.6 C	153.0 C	152.3 C
10	110.3 C	112.1 C	106.9 C	118.3 C	117.8 C
11	64.1 CH_2	67.2 CH_2	63.2 CH_2		
1'	109.5 C	107.1 C	109.5 C	127.4 C	124.5 C
2'	149.6 C	149.7 C	149.4 C	110.5 CH	112.6 CH
3'	99.2 CH	99.3 CH	99.2 CH	148.4 C	148.9 C
4'	149.4 C	148.7 C	149.6 C	148.3 C	149.1 C
5'	142.4 C	142.9 C	142.5 C	108.8 CH	111.2 CH
6'	106.0 CH	107.2 CH	105.5	123.2 CH	121.0 CH
1"/1a"	115.8 CH	116.4 CH	38.4 CH_2	66.8 CH_2	66.4 CH_2
2"/2a"	129.1 CH	130.1 CH	117.4 CH	120.0 CH	118.6 CH
3"/3a"	78.6 C	78.6 C	135.7 C	139.2 C	139.4 C
4"/4a"	28.6 CH_3	28.6 CH_3	25.9 CH_3	25.8 CH_3	25.1 CH_3
5"/5a"	28.3 CH_3	28.1 CH_3	18.0 CH_3	18.3 CH_3	18.5 CH_3
1b"			39.2 CH_2		
2b"			116.3 CH		
3b"			135.6 C		
4b"			25.4 CH_3		
5b"			17.8 CH_3		
OCH_3-6	56.5 CH_3	56.5 CH_3	55.8 CH_3	56.3 CH_3	56.5 CH_3

Pos.	1[b]	2[c]	3[b]	4[c]	5[b]
OCH_3-3'					56.1 CH_3
OCH_3-4'					56.1 CH_3
OCH_2O-3',4'				102.1 CH_2	
OCH_2O-4',5'	101.5 CH_2	102.1 CH_2	101.6 CH_2		

[a] CH_3, CH_2, CH, and C multiplicities were determined by DEPT 90, DEPT 135, and HSQC experiments

[b] Data (δ) measured in $CDCl_3$ at 100.61 MHz (Bruker DRX) and referenced to the solvent residual peak at δ 77.16 [21]

[c] Data (δ) measured in acetone-d_6 at 176.05 MHz (Bruker DRX) and referenced to the solvent residual peak at δ 29.84 [21]

Table 4

Cytotoxicity and NF-κB and K-Ras inhibition of compounds isolated from *M. caeruleaa*.

Compound	Cytotoxicity[b]	NF-κB p65 inhibition[c]	K-Ras inhibition[d]
1	>10	>10	9.4
6	0.1	5.3	3.1
7	0.3	>10	>10
8	>10	>10	3.7
Paclitaxel[e]	0.0008		
Rocaglamide[e]		0.075	
Methyl Rocaglate[e]			0.028

[a] IC_{50} values are the concentration required for 50% inhibition of cell viability after 72 h of incubation with a given test compound and were calculated using nonlinear regression analysis with measurements performed in triplicate and representative of three independent experiments in which the values generally agreed within 10%

[b] Represented as IC_{50} values (μM) toward the HT-29 human colon cancer cell line

[c] Represented as IC_{50} values (μM) for NF-κB inhibition in HeLa cells

[d] Represented as IC_{50} values (μM) for K-Ras inhibition in HT-29 cells

[e] Positive control

Table 5

Quinone reductase induction of compounds isolated from *M. caerulea*[a].

Compound	CD[b]	IC_{50}[c]	CI[d]
1	19.8	>40	>2.4
2	2.2	17.8	8.1
3	2.4	>40	>16.8
8	1.8	35.0	19.4
11	6.6	>40	>7.1
L-sulforaphane[e]	0.51	20.9	40.8

[a]Data are represented as CD or IC_{50} values (μM, toward Hepa 1c1c7 cell line) and were calculated using nonlinear regression analysis with measurements performed in duplicate and representative of two independent readings in which the values generally agreed within 10%

[b]The concentration required to double quinone reductase activity

[c]The concentration that inhibits 50% cell growth

[d]The chemopreventive index (IC_{50}/CD)

[e]Positive control